ISSN 0020-1685, Inorganic Materials, 2008, Vol. 44, No. 10, pp. 1060–1065. © Pleiades Publishing, Ltd., 2008.
Original Russian Text ©M.B. Babanly, G.B. Dashdieva, F.N. Guseinov, 2008, published in Neorganicheskie Materialy, 2008, Vol. 44, No. 10, pp. 1187–1192.

Phase Equilibria in the System Tl_2Te–SnTe–$TlBiTe_2$*

M. B. Babanly, G. B. Dashdieva, and F. N. Guseinov
Baku State University, ul. Khalilova 23, Baku, AZ1148 Azerbaijan
e-mail: babanly_mb@rambler.ru
Received September 14, 2007

Abstract—The phase equilibria in the system Tl_2Te–SnTe–$TlBiTe_2$ (A) have been studied using differential thermal analysis, x-ray diffraction, and microhardness measurements. We have constructed the *T–x* phase diagrams along the SnTe–$TlBiTe_2$, SnTe–Tl_9BiTe_6, and Tl_4SnTe_3–$TlBiTe_2$ joins, the 600- and 800-K sections of the phase diagram of system A, and its liquidus diagram. The results demonstrate that the system contains broad ranges of Tl_5Te_3-structured and SnTe-based solid solutions (δ and γ_1 phases, respectively). There are also relatively small fields of the Tl_2Te-based phase (α) and low- and high-temperature $TlBiTe_2$-based solid solutions (γ_2 and γ_2'). The liquidus surface of system A comprises the primary crystallization fields of the δ, γ_1, and γ_2' phases. The liquidus of the α phase is degenerate. The ternary eutectic between the δ, γ_1, and γ_2' phases melts at 755 K.

DOI: 10.1134/S0020168508100063

INTRODUCTION

Tellurides of heavy *p*-metals are thought to be attractive hosts for the preparation of new thermoelectric materials [1, 2]. In this family of compounds, tin, bismuth, and thallium tellurides are of considerable practical importance [1–5]. One way of enhancing the performance of thermoelectric materials is by utilizing multicomponent compounds with complex structures [2, 6]. The key to the targeted synthesis of new multicomponent tellurides of the above elements lies in knowing the phase equilibria in the corresponding systems.

This led us to study the phase equilibria in the composition region Tl_2Te–SnTe–$TlBiTe_2$ (A) of the quaternary system Tl–Sn–Bi–Te. The constituent binary tellurides Tl_2Te and SnTe melt congruently at 698 and 1080 K, respectively [1, 7, 8]. Tl_2Te has a monoclinic structure [9], and SnTe has a primitive cubic unit cell [7]. The ternary compound $TlBiTe_2$ exists in two crystalline polymorphs. At 780 K, the low-temperature, orthorhombic phase transforms into the high-temperature, disordered phase of variable composition, which melts congruently at 830 K [10–12].

The constituent binaries of system A have been studied by several groups. The Tl_2Te–SnTe system was reported to contain a ternary compound of composition Tl_4SnTe_3, which has a broad homogeneity range (12–40 mol % SnTe) and melts congruently at 825 K [13, 14]. This compound, as well as related solid solutions (δ phase), crystallizes in tetragonal symmetry (Tl_5Te_3 structure, sp. gr. *I*4/*mcm*). The lattice parameters of Tl_4SnTe_3 are a = 8.82 Å and c = 13.01 Å (Z = 4) [15]. The Tl_2Te–$TlBiTe_2$ system contains a compound of composition Tl_9BiTe_6, which melts congruently at 830 K, also has a tetragonal structure of the Tl_5Te_3 type (a = 8.855 Å, c = 13.048 Å, Z = 2) [10, 16], and forms a continuous series of solid solutions with Tl_2Te [10].

As shown by Mazelsky and Lubell [17], the SnTe–$TlBiTe_2$ system contains limited solid solutions based on SnTe (56 mol %) and $TlBiTe_2$ (21 mol %).

Dashdieva et al. [18] studied the phase equilibria in the composition region Tl_2Te–Tl_4SnTe_3–Tl_9BiTe_6 of system A. According to their results, the Tl_4SnTe_3-Tl_9BiTe_6 join is pseudobinary, with a continuous series of Tl_5Te_3-structure solid solutions (δ phase). Their lattice parameters follow Vegard's law (a = 8.821–8.854 Å, c = 13.01–13.05 Å). The δ phase field extends over most of the Tl_2Te–Tl_4SnTe_3–Tl_9BiTe_6 system [18].

EXPERIMENTAL

The constituent tellurides of system A were synthesized by melting appropriate high-purity elemental mixtures in silica tubes sealed off under a vacuum of ~10^{-2} Pa, followed by slow cooling. The synthesis temperature was 750 (Tl_2Te), 1150 (SnTe), or 900 K ($TlBiTe_2$), that is, slightly above the corresponding melting point. The synthesized compounds were identified by differential thermal analysis (DTA) and x-ray diffraction (XRD).

* Presented in part at the XII Conference *High-Purity Substances and Materials: Preparation, Analysis, and Application*, Nizhni Novgorod, Russia, May 28–31, 2007.

Alloys of system A were prepared by vacuum-melting telluride mixtures. We prepared SnTe–$TlBiTe_2$, Tl_4SnTe_3-$TlBiTe_2$, and SnTe–Tl_9BiTe_6 alloys and a number of alloys beyond these joins. Using DTA results for a number of unhomogenized alloys and earlier data [10, 13, 18], we selected heat-treatment temperatures at which the alloys were equilibrated for 500 h. The alloys annealed at 600 K were furnace-cooled, and those annealed at 800 K were quenched in cold water.

The alloys were characterized by DTA (NTR-74 pyrometer, Chromel–Alumel thermocouples), XRD (DRON-2 powder diffractometer, CuK_α radiation), and microhardness measurements (PMT-3 tester, 0.2-N indentation load).

RESULTS AND DISCUSSION

The present experimental data and earlier results [10, 13, 14, 18] for the constituent binaries and the Tl_2Te–Tl_4SnTe_3–$TlBi_6Te_2$ system are summarized in Figs. 1–6.

The present *T–x* phase diagram of the SnTe–$TlBiTe_2$ system (Fig. 1a) differs somewhat from that reported by Mazelsky and Lubell [17]. According to our results, this system involves both eutectic and eutectoid phase relations. The eutectic (e_1) is located at ≃85 mol % $TlBiTe_2$, with a melting point of 815 K.

The homogeneity range of the SnTe-based phase (γ_1 phase) extends to 80 mol % $TlBiTe_2$ at 800 K and to 72 mol % $TlBiTe_2$ at 600 K. The formation of low- and high-temperature $TlBiTe_2$-based solid solutions (γ_2- and γ_2' phases) is accompanied by a reduction in the temperature of the polymorphic transformation from 765 to 750 K and a transition to eutectoid phase relations. The eutectoid point (e_2) is located at ≃90 mol % $TlBiTe_2$ and 750 K (Fig. 1a). The width of the homogeneity range of the γ_2' phase is 10 mol % (800 K), and that of the γ_2 phase is ≃5 mol % (600 K).

XRD and microhardness data are consistent with the *T–x* phase diagram of the SnTe–$TlBiTe_2$ system. Powder XRD patterns of the alloys containing 0–70 mol % $TlBiTe_2$ (annealing at 600 K) or 0–80 mol % $TlBiTe_2$ (quenching after annealing at 800 K) show only reflections from an SnTe-based cubic phase, and its lattice parameter varies almost linearly with composition, from a = 6.327 (SnTe) to 6.465 Å (80 mol % $TlBiTe_2$) (Fig. 1c). The microhardness H of the γ_1 phase rises steadily from ≃850 (SnTe) to ≃1400 MPa (80 mol % $TlBiTe_2$), and that of the γ_2 phase rises from ≃500 ($TlBiTe_2$) to 600 MPa (95 mol % $TlBiTe_2$). The microhardness of the samples quenched from 800 K slightly exceeds that of the corresponding samples annealed at 600 K (Fig. 1b).

The XRD, DTA, and microhardness data for the alloys annealed at 600 K were used to map out the subsolidus phase diagram of system A (Fig. 2). As seen in

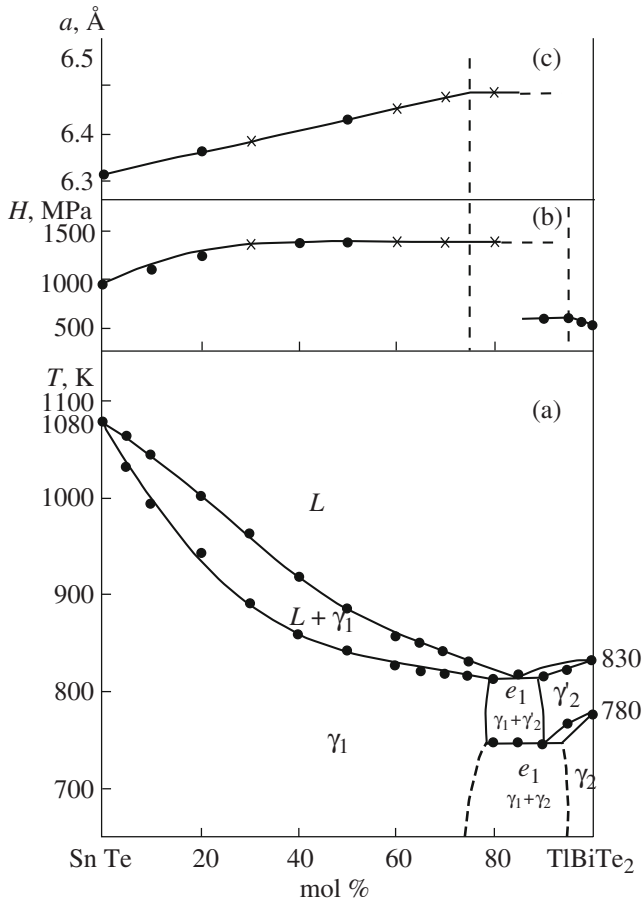

Fig. 1. *T–x* phase diagram of the SnTe–$TlBiTe_2$ system (a); composition dependences of the microhardness (b) and lattice parameter (c). The crosses in panels b and c represent samples quenched from 800 K.

Fig. 2, the 600-K section comprises single- (δ, γ_1, and γ_2), two-, and three-phase fields. The γ_1 and γ_2 phase fields extend along the constituent binary SnTe–$TlBiTe_2$ and are 2–3 mol % in width. The δ phase field extends over most of the Tl_2Te–Tl_4SnTe_3–Tl_9BiTe_6 region. In addition, there are two fields (α and X) near Tl_2Te. The alloys in the α field are isostructural with Tl_2Te. We failed to detect an $\alpha + \delta$ two-phase field, which leads us to assume that the $\alpha \rightleftarrows \delta$ phase transformation is morphotropic. In the X field, the Tl_2Te–SnTe–$TlBiTe_2$ plane is unstable: the equilibrium alloys contain, in addition to the α and δ phases, a Tl-based metallic phase [18]. This rare effect, also encountered in the constituent system Tl_2Te–SnTe, was analyzed in detail elsewhere [13, 14].

The phase diagram of the SnTe–Tl_9BiTe_6 system (Fig. 3) is similar in appearance to that of a pseudobinary eutectic, but this system is not pseudobinary. The alloys of this system consist of two phases, $\gamma_1 + \delta$, but, as seen in Fig. 2, the compositions of the equilibrium γ_1 and δ phases lie beyond this join. Comparison of Figs. 3

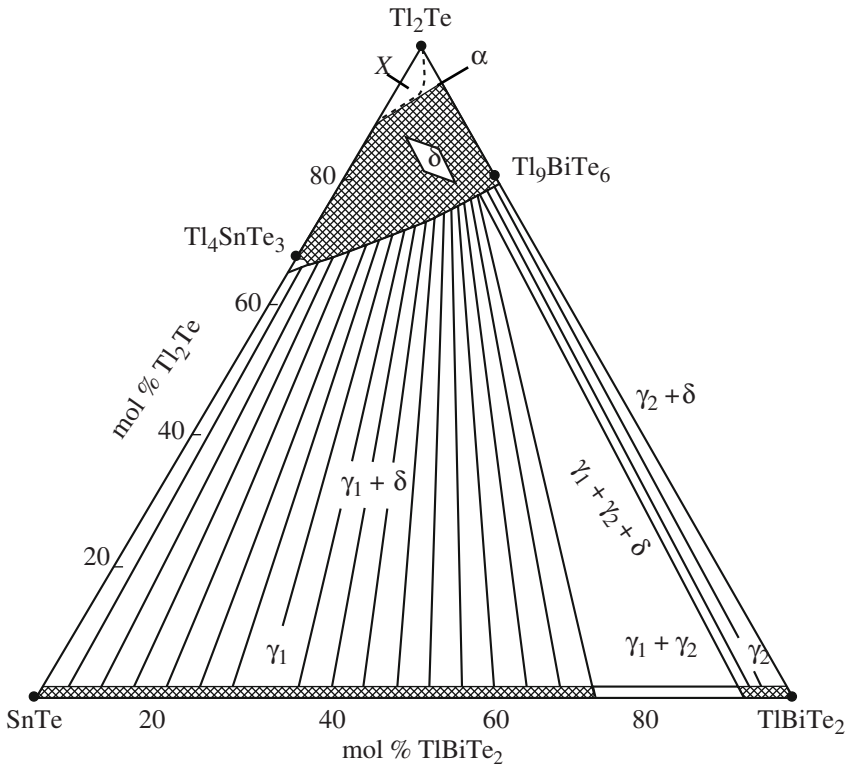

Fig. 2. 600-K section of the *T–x–y* phase diagram of the Tl_2Te–SnTe–$TlBiTe_2$ system.

and 5 demonstrates that the SnTe–Tl_9BiTe_6 join passes through primary crystallization fields and intersects the eutectic curve e_2E, representing the univariant equilibrium

$$L \rightleftharpoons \gamma_1 + \delta. \quad (1)$$

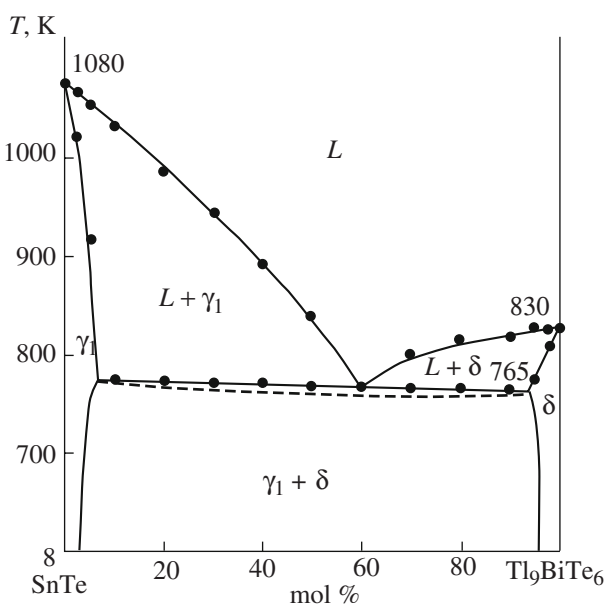

Fig. 3. *T–x* phase diagram of the SnTe–Tl_9BiTe_6 system.

Because of the very small slope of the e_2E curve over the SnTe–Tl_9BiTe_6 join, this eutectic transformation occurs in a very narrow temperature range, and is represented by a single, sharp DTA peak. For this reason, the $L + \gamma_1 + \delta$ field in Fig. 3 is marked by a dashed line. Along this join, the homogeneity ranges of the γ_1 and δ phases are ≃3–4 mol % in width (600 K).

More complex phase relations were found along the Tl_4SnTe_3-$TlBiTe_2$ join (Fig. 4), which passes through five phase fields below the solidus (Fig. 2). Its liquidus comprises three branches, corresponding to the primary crystallization of the δ-, γ_1-, and γ_2' phases, which are separated by the eutectic curves e_1E and e_2E (Fig. 5). The 755-K horizontal represents the four-phase equilibrium

$$L_E \rightleftharpoons \gamma_1 + \gamma_2' + \delta, \quad (2)$$

and the 748-K horizontal represents the eutectoid equilibrium

$$\gamma_2' \rightleftharpoons \gamma_1 + \gamma_2 + \delta. \quad (3)$$

Below this horizontal, the alloys containing 50–87 mol % $TlBiTe_2$ consist of three phases: $\gamma_1 + \gamma_2 + \delta$ (Fig. 2). In the composition ranges ≃7–50 and 80–90 mol % $TlBiTe_2$, the solidus line represents the univariant eutectic processes (1) and (4), respectively:

$$L_E \rightleftharpoons \gamma_2' + \delta. \quad (4)$$

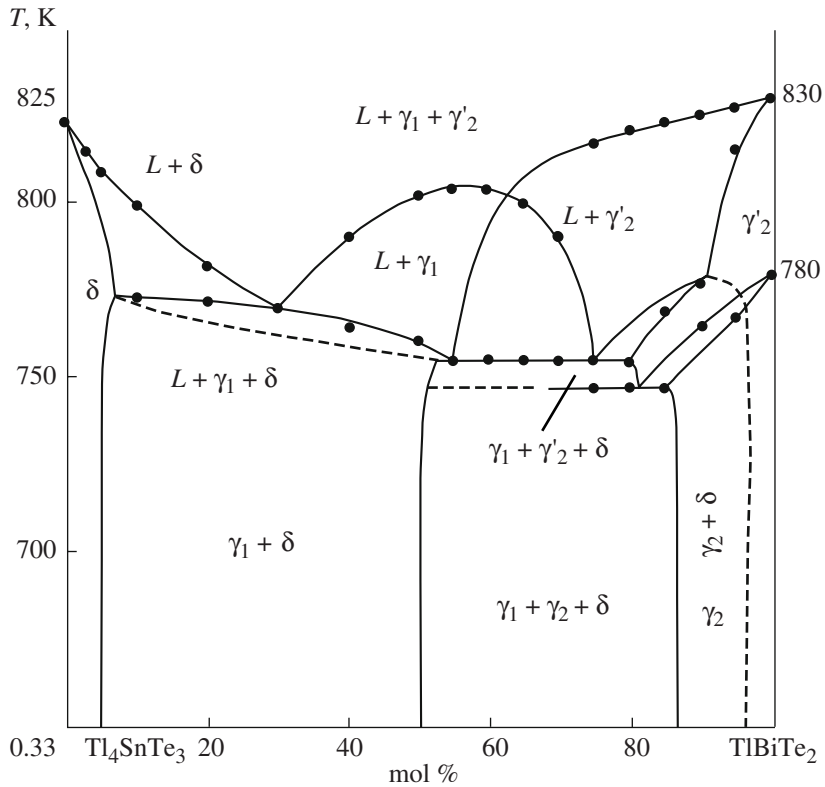

Fig. 4. *T–x* phase diagram of the Tl_4SnTe_3–$TlBiTe_2$ system.

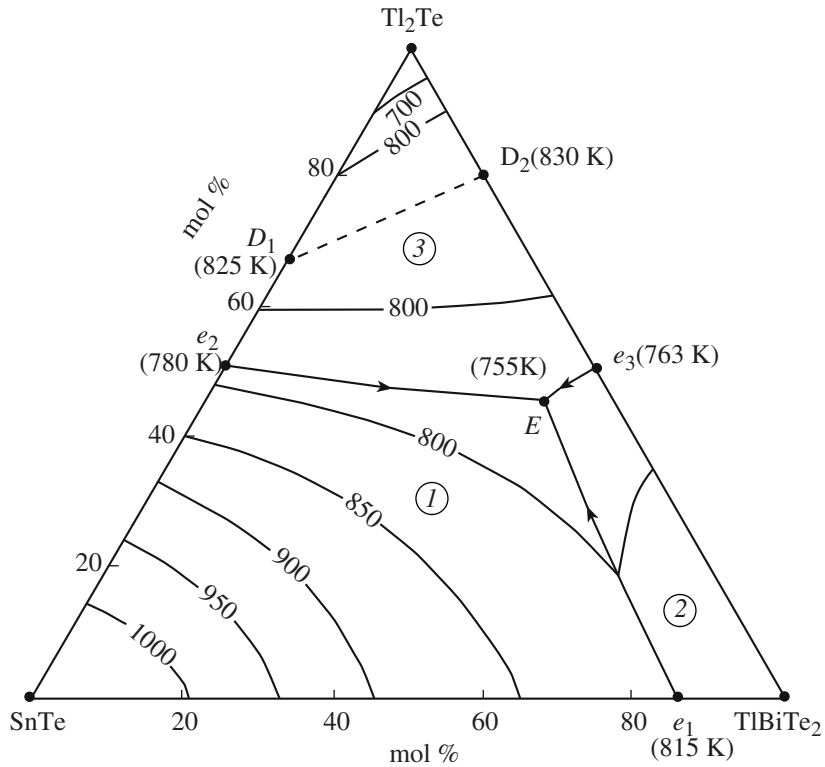

Fig. 5. Liquidus diagram of the Tl_2Te–SnTe–$TlBiTe_2$ system. Primary crystallization fields: (*1*) γ_1, (*2*) γ'_2, (*3*) δ. The dashed line represents the pseudobinary join Tl_4SnTe_3–Tl_9BiTe_6.

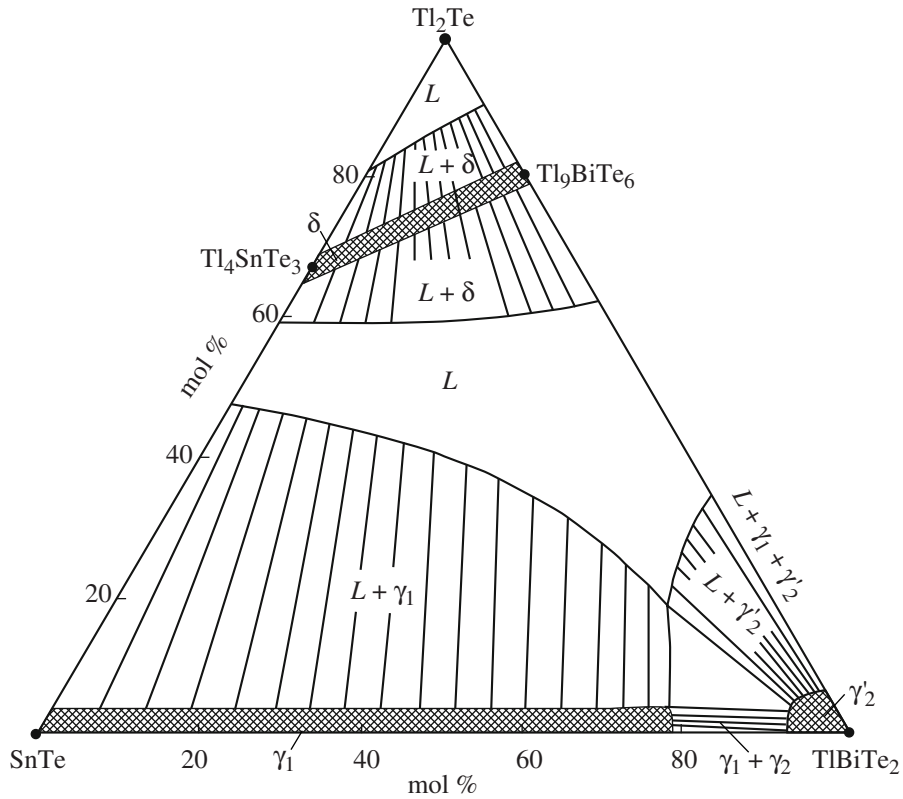

Fig. 6. 800-K section of the Tl_2Te–SnTe–$TlBiTe_2$ phase diagram.

The homogeneity ranges of the δ and γ_2 phases along the Tl_4SnTe_3-$TlBiTe_2$ join are no wider than 5 mol %.

The liquidus surface of system A comprises three primary crystallization fields, those of the δ-, γ_1-, and γ'_2 phases (Fig. 5). The eutectic curves e_2E, e_3E, and e_1E, separating these fields, represent the univariant equilibria (1), (4), and

$$L_{e_1E} \rightleftharpoons \gamma_1 + \gamma'_2.$$

The ternary eutectic point E is located at ≃45 mol % Tl_2Te and ≃10 mol % SnTe.

The dashed line in Fig. 5 represents the only pseudobinary join (Tl_4SnTe_3–Tl_9BiTe_6) in system A. The liquidus surface of the Tl_2Te-based phase (α) is degenerate.

Figure 6 shows the isothermal section of the phase diagram of system A inferred from the data for alloys quenched after 800-K annealing and from the position of the corresponding isotherms in Fig. 5. From the position of tie lines in the two-phase regions $L + \gamma_1$, $L + \gamma'_2$, and L + δ, one can select melt compositions for the crystal growth of solid solutions of controlled composition by directional solidification.

REFERENCES

1. Shelimova, L.E., Tomashik, V.N., and Grytsiv, V.I., *Diagrammy sostoyaniya v poluprovodnikovom materialovedenii* (Phase Diagrams in Semiconductor Materials Research), Moscow: Nauka, 1991.
2. Shelimova, L., Karpinskii, O.G., and Zemskov, V.S., Promising Thermoelectric Materials Based on Layered Tetradymite-Like Chalcogenides, *Perspekt. Mater.*, 2000, no. 5, pp. 23–32.
3. Karpinskii, O.G., Shelimova, L.E., Kretova, M.A., et al., X-Ray Diffraction Study of Mixed-Layer Compounds in the Pseudobinary System SnTe–Bi_2Te_3, *Neorg. Mater.*, 2003, vol. 39, no. 3, pp. 305–311 [*Inorg. Mater.* (Engl. Transl.), vol. 39, no. 3, pp. 240–246].
4. Wolfing, B., Kloc, C., Teubner, J., and Bucher, E., High Performance Thermoelectric Tl_9BiTe_6 with an Extremely Low Thermal Conductivity, *Phys. Rev. Lett.*, 2001, vol. 36, no. 19, pp. 4350–4353.
5. Yamanaka, Sh., Kosuka, A., and Korosaki, K., Thermoelectric Properties of Tl_9BiTe_6, *J. Alloys Compd.*, 2003, vol. 352, pp. 275–278.
6. Ioffe, A.F., *Poluprovodnikovye termoelementy* (Semiconductor Thermoelements), Moscow: Akad. Nauk SSSR, 1960.
7. *Fiziko-khimicheskie svoistva poluprovodnikovykh veshchestv. Spravochnik* (Physicochemical Properties of Semiconductors: A Handbook) Novoselova, A.V. and Lazarev, V.B., Eds., Moscow: Nauka, 1976.

8. Asadov, M.M., Babanly, M.B, and Kuliev, A.A., Phase Equilibria in the Tl–Te System, *Izv. Akad. Nauk SSSR, Neorg. Mater.*, 1977, vol. 13, no. 8, pp. 1407–1410.

9. Cerny, R., Joubert, J.M., Filinchik, Y., and Feutelais, Y., Tl_2Te and Its Relationship with Tl_5Te_3, *Acta Crystallogr., Sect. C: Cryst. Struct. Commun.*, 2002, vol. 58, no. 5, pp. 163–165.

10. Babanly, M.B., Akhmad'yar, A., and Kuliev, A.A., System Tl_2Te–Bi_2Te_3–Te, *Zh. Neorg. Khim.*, 1985, vol. 30, no. 9, pp. 2356–2361.

11. Pradel, A., Tedenac, J.C., Brun, G., and Maurin, M., Mise au point dans le ternaire Tl–Bi–Te. Existence de deux phases nonstoechiometriques de type $TlBiTe_2$, *J. Solid State Chem.*, 1982, vol. 5, no. 1, pp. 99–111.

12. Voroshilov, Yu.V., Evstigneeva, T.A., and Nekrasov, I.Ya., *Kristallokhimicheskie tablitsy troinykh khal'-kogenidov* (Crystal-Chemical Tables for Ternary Chalcogenides), Moscow: Nauka, 1989.

13. Gotuk Ali Alarik, Babanly, M.B., and Kuliev, A.A., Phase Equilibria in the Systems Tl_2Te–SnTe and Tl_2Te–PbTe, *Uch. Zap. MV SSO Az. SSR, Ser Khim. Nauk*, 1978, no. 3, pp. 30–32.

14. Gotuk Ali Alarik, Babanly, M.B., and Kuliev, A.A., Phase Equilibria in the System Tl–Sn–Te, *Izv. Akad. Nauk SSSR, Neorg. Mater.*, 1979, vol. 15, no. 8, pp. 1356–1361.

15. Bradtmöller, S. and Böttcher, P., Darstellung und Kristallstruktur von $SnTl_4Te_3$ und $PbT_{l4}Te_3$, *Z. Anorg. Allg. Chem.*, 1993, vol. 619, pp. 1155–1160.

16. Doert, T. and Böttcher, P., Crystal Structure of Bismuthnonathallium Hexatelluride $BiTl_9Te_6$, *Z. Kristallogr.*, 1994, vol. 209, p. 95.

17. Mazelsky, R. and Lubell, M.S., Solid Solution Study of Some Post-Transition Metal Tellurides of the Rock Salt Structural Type, *J. Phys. Chem.*, 1962, vol. 66, no. 8, pp. 1408–1411.

18. Dashdieva, G.B., Guseinov, F.N., and Babanly, M.B., Phase Equilibria in the System Tl_2Te–Tl_4SnTe_3–Tl_9BiTe_6, *Vestn. Bakinsk. Univ., Ser. Estestv. Nauk*, 2007, no. 1, pp. 38–42.